

# Relativistic QRPA description of isoscalar compression modes in open-shell nuclei in the $A \approx 60$ mass region

N. Paar\*

*Institut für Kernphysik, Technische Universität Darmstadt,  
Schlossgartenstrasse 9, D-64289 Darmstadt, Germany and  
Physics Department, Faculty of Science, University of Zagreb, Croatia*

D. Vretenar and T. Nikšić

*Physics Department, Faculty of Science, University of Zagreb, Croatia*

P. Ring

*Physik-Department der Technischen Universität München, D-85748 Garching, Germany*

(Dated: November 24, 2018)

arXiv:nucl-th/0606054v1 27 Jun 2006

---

\* Electronic address: nils.paar@physik.tu-darmstadt.de

## Abstract

Very recent inelastic  $\alpha$ -scattering data on the isoscalar monopole and dipole strength distributions in  $^{56}\text{Fe}$ ,  $^{58}\text{Ni}$ , and  $^{60}\text{Ni}$  are analyzed in the relativistic quasiparticle random-phase approximation (RQRPA) with the DD-ME2 effective nuclear interaction (nuclear matter compression modulus  $K_{nm} = 251$  MeV). In all three nuclei the calculation nicely reproduces the observed asymmetric shapes of the monopole strength, and the bimodal structure of the dipole strength distributions. The calculated centroid and mean energies are in very good qualitative agreement with the experimental values both for the monopole, and for the low- and high-energy components of the dipole transition strengths. It is noted, however, that while DD-ME2 reproduces in detail the excitation energies of the giant monopole resonances (GMR) in nuclei with  $A \geq 90$ , the theoretical centroids are systematically above the experimental values in lighter nuclei with  $A \leq 60$ . The latter can be reproduced with an effective interaction with a lower value of  $K_{nm} \approx 230$  MeV but, because of the asymmetric shapes and pronounced fragmentation of the monopole strength distributions, isoscalar GMR data in light nuclei cannot provide accurate estimates of the nuclear matter compression modulus.

PACS numbers: 21.60.Ev, 21.60.Jz, 21.65.+f, 24.30.Cz

Experimental excitation energies of compressional (monopole and dipole) vibrational modes in atomic nuclei can in principle be used to deduce the value of the nuclear matter compression modulus  $K_{nm}$  [1]. This quantity is related to the curvature of the nuclear matter equation of state at the saturation point, and controls basic properties of atomic nuclei, the structure of neutron stars, the dynamics of heavy-ion collisions and of supernovae explosions. The nuclear matter compressibility cannot be measured directly, but rather deduced from a comparison of experimental excitation energies of isoscalar giant monopole resonances (ISGMR), with the corresponding values predicted by microscopic nuclear effective interactions characterized by different values of  $K_{nm}$ .

Inelastic  $\alpha$ -scattering experiments have been used in high precision studies of the systematics of ISGMR in nuclei with  $A \geq 90$ . Nuclear structure models provide a consistent description of the shapes of strength distributions and the mass dependence of excitation energies, and thus relate the ISGMR to the nuclear compressibility and to the nuclear matter compression modulus. There is much less experimental information, and only few microscopic theoretical analyses of the structure of compressional modes in lighter nuclei with  $A < 90$ . While in heavy nuclei the shape of the ISGMR strength distribution is typically symmetric, for  $A < 90$  the ISGMR display asymmetric shapes with a slower slope on the high energy side of the peak, and with a further decrease of the mass number the ISGMR strength distributions become strongly fragmented. An interesting question, of course, is whether studies of compressional vibrations in lighter nuclei can provide additional information on the nuclear matter compression modulus. Namely,  $K_{nm}$  corresponds to bulk nuclear compressibility, whereas one expects that surface compressibility plays an increasingly important role in the structure of ISGMR in lighter systems. In a very recent study [2] isoscalar giant resonances in  $^{56}\text{Fe}$ ,  $^{58}\text{Ni}$ , and  $^{60}\text{Ni}$  have been studied with small-angle inelastic  $\alpha$ -scattering. In particular, most of the expected isoscalar E0 has been identified below 40 MeV excitation energy, and between 56% and 72% of the isoscalar E1 strength has been located in these nuclei. It was noted, however, that there are no specific microscopic calculations of E0 and E1 strength distributions in  $^{56}\text{Fe}$  and  $^{60}\text{Ni}$ . The mass dependence of the ISGMR excitation energies between  $A = 40$  and  $A = 90$  was thus compared with results of leptodermous expansions based on Hartree-Fock + RPA calculations with Skyrme interactions [3], and constrained relativistic mean-field calculations [4]. The purpose of this work is to perform fully self-consistent relativistic quasiparticle random-phase approxima-

tion (RQRPA) calculations of isoscalar E0 and E1 strength distributions in  $^{56}\text{Fe}$ ,  $^{58}\text{Ni}$ , and  $^{60}\text{Ni}$ , using a modern effective density-dependent interaction which is known to reproduce the systematics of compressional modes in heavier nuclei with  $A \geq 90$ .

Theoretical studies of nuclear compressional modes in the last decade have employed the fluid dynamics approach [5], the Hartree-Fock plus random phase approximation (RPA) [6, 7, 8, 9], the RPA based on separable Hamiltonians [10], linear response within a stochastic one-body transport theory [11], the relativistic transport approach [12], and the self-consistent relativistic RPA [13, 14, 15, 16]. As has been pointed out by Shlomo et al., however, most current implementations of the non-relativistic RPA are not self-consistent, and based on numerous approximations [17]. Very recent studies have emphasized the importance of a fully self-consistent description of ISGMR, and confirmed that the low value of  $K_{nm} = 210\text{--}220$  MeV, previously obtained with Skyrme functionals, is an artefact of the inconsistent implementation of effective interactions [9, 18]. The excitation energies of the ISGMR in heavy nuclei are thus best described with Skyrme and Gogny effective interactions with  $K_{nm} \approx 235$  MeV. In Ref. [8] it has been shown that it is also possible to construct Skyrme forces that fit nuclear ground state properties and reproduce ISGMR energies, but with  $K_{nm} \approx 255$  MeV. In Ref. [9] a new set of Skyrme forces was constructed that spans a wider range of values of  $K_{nm}$  and the symmetry energy at saturation density  $a_4$ . RPA calculations with these forces have shown that the ISGMR data are best reproduced with  $K_{nm} = 230\text{--}240$  MeV, whereas higher values of  $K_{nm}$  would require unrealistically large value of  $a_4$ . On the other hand, it appears that in the relativistic framework the interval of allowed values for  $K_{nm}$  is more restricted. A recent relativistic RPA analysis based on modern effective Lagrangians with explicit density dependence of the meson-nucleon vertex functions, has shown that only effective interactions with  $K_{nm} = 250\text{--}270$  MeV reproduce the experimental excitation energies of ISGMR in medium-heavy and heavy nuclei, and that  $K_{nm} \approx 250$  MeV represents the lower limit for the nuclear matter compression modulus of relativistic mean-field interactions [16].

Data on the compressional isoscalar giant dipole resonance (ISGDR) could also be used to constrain the range of allowed values of  $K_{nm}$  [19, 20]. The problem, however, is that the isoscalar E1 strength distributions display a characteristic bimodal structure with two broad components: one in the low-energy region close to the isovector giant dipole resonance (IVGDR) ( $\approx 2\hbar\omega$ ), and the other at higher energy close to the electric octupole resonance

( $\approx 3\hbar\omega$ ). Theoretical analyses have shown that only the high-energy component represents compressional vibrations [21, 22], whereas the broad structure in the low-energy region corresponds to vortical nuclear flow associated with the toroidal dipole moment [23, 24, 25]. However, as has also been pointed out in the recent study of the interplay between compressional and vortical nuclear currents [24], a strong mixing between compressional and vorticity vibrations in the isoscalar E1 states can be expected up to the highest excitation energies in the region  $\approx 3\hbar\omega$ . Nevertheless, models which use effective interactions with  $K_{nm}$  adjusted to ISGMR excitation energies in heavy nuclei, also reproduce the structure of the high-energy portion of ISGDR data [17, 26, 27].

In this work the isoscalar E0 and E1 strength distributions for the open-shell nuclei  $^{56}\text{Fe}$ ,  $^{58}\text{Ni}$ , and  $^{60}\text{Ni}$  are calculated in the relativistic quasiparticle random-phase approximation (RQRPA), formulated in the canonical single-nucleon basis of the relativistic Hartree-Bogoliubov (RHB) model [28]. The RQRPA model is fully self-consistent: the same interactions, in the particle-hole and particle-particle channels, are used both in the RHB equations that determine the canonical quasiparticle basis, and in the RQRPA equations. In both channels the same strength parameters of the interactions are used in the RHB and RQRPA calculations. This is an essential feature of the RHB+RQRPA approach and it ensures that RQRPA amplitudes do not contain spurious components associated with the mixing of the nucleon number in the RHB ground state, or with the center-of-mass translational motion.

In Fig. 1 we display the isoscalar monopole strength distributions for  $^{56}\text{Fe}$ ,  $^{58}\text{Ni}$ , and  $^{60}\text{Ni}$ . The RHB+RQRPA calculation has been performed with the DD-ME2 effective interaction [29] in the particle-hole channel and, as in most applications of the RHB model [30], the finite-range Gogny force has been used in the particle-particle channel. DD-ME2 belongs to a new class of relativistic effective nuclear interactions with density-dependent meson-nucleon vertex functions. In a number of recent studies it has been shown that this type of effective interactions provides a realistic description of asymmetric nuclear matter, neutron matter and finite spherical and deformed nuclei. These interactions allow for a softer equation of state of nuclear matter (i.e. lower incompressibility) and a lower value of the symmetry energy at saturation. In addition to nuclear matter and ground-state properties of spherical nuclei, the parameters of DD-ME2 have been adjusted to the excitation energies of the ISGMR and IVGDR in  $^{208}\text{Pb}$ . For DD-ME2 the nuclear matter compression modulus

amounts  $K_{nm} = 251$  MeV. The strength distributions in Fig. 1 can be compared with the data from Ref. [2] (Figs. 8, 9 and 10). In all three nuclei the calculation predicts asymmetric shapes for the isoscalar E0 strength distributions, in agreement with data. In particular, an additional tail in the transition strength is obtained above the main ISGMR peaks for  $^{56}\text{Fe}$  and  $^{60}\text{Ni}$ . For  $^{58}\text{Ni}$  most of the strength is distributed over two major peaks, with an additional pronounced high-energy tail. The arrows denote the positions of the experimental centroid ( $\bar{E}_1 = m_1/m_0$ ) and mean energies ( $\bar{E}_3 = \sqrt{m_3/m_1}$ ), where  $m_k = \int E^k R(E)dE$  are the energy moments, and  $R(E)$  is the transition strength distribution function. We note that in all three nuclei the main ISGMR peak predicted by the RQRPA calculation is located in the narrow energy window between the  $\bar{E}_1$  and  $\bar{E}_3$  experimental energies.

In the upper panel of Fig. 2 we plot the RHB+RQRPA results for the ISGMR centroid energies ( $m_1/m_0$ ) of a series of spherical nuclei from  $^{40}\text{Ca}$  to  $^{208}\text{Pb}$ , calculated with the DD-ME2 effective interaction, in comparison with data from the Texas A&M University (TAMU) [2, 31, 32, 33] and Osaka [26, 27] compilations. We note that the latter data correspond to peak energies and, especially in nuclei in which a high-energy tail is found above the main peak, these values should be somewhat below the TAMU centroid energies. The agreement between the excitation energies calculated with DD-ME2 and the TAMU data is remarkable for nuclei with  $A \geq 90$ , whereas the theoretical centroids are systematically above the experimental values in lighter nuclei. The origin of this discrepancy is not understood, but it could be due to the fact that in light nuclei the surface incompressibility plays a more important role in determining the ISGMR, whereas  $K_{nm}$  represents the volume incompressibility. The former quantity is seldom taken into account when adjusting the parameters of an effective interaction and, therefore, we do not really expect that DD-ME2 can reproduce in detail the moments of asymmetric and even fragmented isoscalar E0 strength distributions in light nuclei with  $A \leq 60$ .

It seems that data on ISGMR in light nuclei are not very useful in extracting information on the nuclear matter compression modulus  $K_{nm}$ . Nevertheless, we have tried to reproduce these data with few additional effective interactions. In the recent analysis of nuclear matter incompressibility in the relativistic mean-field framework [16], families of density-dependent interactions with different values of the nuclear matter compression modulus  $K_{nm}$  and symmetry energy at saturation (volume asymmetry)  $a_4$ , were adjusted to reproduce nuclear matter and ground-state properties of spherical nuclei. By performing fully

consistent RRPA/RQRPA calculations of isoscalar E0 and isovector E1 strength distributions in spherical nuclei with  $A \geq 90$ , it has been shown that the comparison with data restricts the values of  $K_{nm}$  to  $\approx 250 - 270$  MeV, and the range of volume asymmetry to  $32 \text{ MeV} \leq a_4 \leq 36 \text{ MeV}$ . A weak correlation between  $a_4$  and  $K_{nm}$  was found, i.e. interactions with lower volume asymmetry allow for slightly lower values of  $K_{nm}$ . Therefore in addition to DD-ME2, the family of interactions with  $a_4 = 32$  MeV and  $K_{nm}=230, 250,$  and  $270$  MeV [16] has been used in a RHB+RQRPA calculation of ISGMR in  $^{40}\text{Ca}$ ,  $^{56}\text{Fe}$ ,  $^{58}\text{Ni}$ ,  $^{60}\text{Ni}$ , and  $^{90}\text{Zr}$ . The resulting mean energies  $\bar{E}_3 = \sqrt{m_3/m_1}$  are plotted in the lower panel of Fig. 2, in comparison with data from Refs. [2, 31, 32]. We notice that while DD-ME2 and the  $K_{nm}=250$  MeV effective interaction reproduce the experimental value  $\bar{E}_3$  for  $^{90}\text{Zr}$ , data in lighter nuclei are better described by the effective interaction with  $K_{nm}=230$  MeV, except possibly for  $^{58}\text{Ni}$ , but for this nucleus the experimental  $\bar{E}_3$  differs considerably from the values in the neighboring  $^{56}\text{Fe}$  and  $^{60}\text{Ni}$  [2].

For the DD-ME2 effective interaction, the RHB+RQRPA isoscalar dipole transition strength distributions in  $^{56}\text{Fe}$ ,  $^{58}\text{Ni}$ , and  $^{60}\text{Ni}$  are shown in Fig. 3. In all three nuclei the E1 strength is strongly fragmented and distributed over a wide range of excitation energy between 10 MeV and 40 MeV, in agreement with the experimental results of Ref. [2]. In the experiment between 56% and 72% of the isoscalar E1 strength has been located in these nuclei below 40 MeV excitation energy, and some missing strength probably lies at higher energies. Similarly to the results obtained for heavier nuclei [21, 22, 25], the E1 strength is basically concentrated in two broad structures: one in the region  $10 \text{ MeV} \leq E_x \leq 20 \text{ MeV}$ , and the high-energy component above 25 MeV and extending above 40 MeV excitation energy. Only the high-energy portion of the calculated E1 strength is sensitive to the nuclear matter compression modulus of the effective interaction. In a number of recent theoretical studies [23, 24, 25] it has been shown that the low-lying E1 strength mostly corresponds to vortical flow (dipole toroidal mode), although a strong mixture of compressional and vortical velocity fields is predicted in the intermediate and high-energy region.

In Fig. 3 the thick arrows denote the locations of the experimental centroid energies ( $m_1/m_0$ ) in the low- and high-energy regions of the isoscalar E1 strength in  $^{56}\text{Fe}$ ,  $^{58}\text{Ni}$ , and  $^{60}\text{Ni}$  [2]. These are compared in Fig. 4 with the theoretical values of the centroids of the low- and high-energy components, for different values of  $E_c$ , the somewhat arbitrary parameter which separates the low- and high-energy regions. We notice a good qualitative agreement

between the calculated and experimental centroids in the high-energy region, especially taking into account that the E1 strength above  $E_x = 40$  MeV has not been observed in the experiment. In the low-energy region, however, the theoretical centroid energies are systematically below the experimental values by  $\approx 1-4$  MeV, depending on the choice of  $E_c$ . This effect is in agreement with previous RRPAs calculations in heavier nuclei [25], and supports the picture of pronounced mixing between compressional and vorticity vibrations in the intermediate region of excitation energies.

In conclusion, we have performed RHB+RQRPA calculations of the isoscalar monopole and dipole strength distributions in  $A \approx 60$  nuclei. The results obtained with the DD-ME2 effective interaction (nuclear matter compression modulus  $K_{nm} = 251$  MeV) have been compared with very recent data on the E0 and E1 strength distribution in  $^{56}\text{Fe}$ ,  $^{58}\text{Ni}$ , and  $^{60}\text{Ni}$  [2]. For the isoscalar monopole resonance we find very good qualitative agreement between theory and experiment, both for the asymmetric shapes of the strength distributions, as well as for centroid ( $\bar{E}_1 = m_1/m_0$ ) and mean energies ( $\bar{E}_3 = \sqrt{m_3/m_1}$ ). It has been noted, however, that while there is an excellent agreement between the ISGMR excitation energies calculated with DD-ME2 and the data for nuclei with  $A \geq 90$ , the theoretical centroids are systematically above the experimental values in lighter nuclei with  $A \leq 60$ . Even though because of asymmetric shapes and pronounced fragmentation, ISGMR data in light nuclei are probably not very useful for extracting information on the nuclear matter compression modulus, we have shown that the ISGMR centroids in nuclei with  $A \leq 60$  are better described with an effective interaction similar to DD-ME2, but with a lower value of  $K_{nm} \approx 230$  MeV. The isoscalar E1 strength distributions calculated with DD-ME2 are in good agreement with the experimental results [2], and reproduce the observed bimodal structure with two broad components in the  $2\hbar\omega$  and  $3\hbar\omega$  energy regions. The calculated centroid energies of the low- and high-energy E1 components in  $^{56}\text{Fe}$ ,  $^{58}\text{Ni}$ , and  $^{60}\text{Ni}$  qualitatively reproduce the experimental values obtained from small-angle inelastic  $\alpha$ -scattering data.

## ACKNOWLEDGMENTS

This work has been supported in part by the Bundesministerium für Bildung und Forschung under project 06 TM 193, by the Gesellschaft für Schwerionenforschung (GSI) Darmstadt, and by the Alexander von Humboldt Stiftung.



- 
- [1] J. P. Blaizot, Phys. Rep. 64, 171 (1980).
- [2] Y.-W. Lui, D. H. Youngblood, H. L. Clark, Y. Tokimoto, and B. John, Phys. Rev. C 73, 014314 (2006).
- [3] R. C. Nayak, J. M. Pearson, M. Farine, P. Gleissl, and M. Brack, Nucl. Phys. A 516, 62 (1990).
- [4] T. v. Chossy and W. Stocker, Phys. Rev. C 56, 2518 (1997).
- [5] V. M. Kolomietz and S. Shlomo, Phys. Rev. C 61, 064302 (2000).
- [6] I. Hamamoto, H. Sagawa, and X. Z. Zhang, Phys. Rev. C 56, 3121 (1997).
- [7] S. Shlomo and A. I. Sanzhur, Phys. Rev. C 65, 044310 (2002).
- [8] B. K. Agrawal, S. Shlomo, and V. Kim Au, Phys. Rev. C 68, 031304(R) (2003).
- [9] G. Colò, N. V. Giai, J. Meyer, K. Bennaceur, and P. Bonche, Phys. Rev. C 70, 024307 (2004).
- [10] J. Kvasil, N. Lo Iudice, Ch. Stoyanov, and P. Alexa, J. Phys. G 29, 753 (2003).
- [11] D. Lacroix, S. Ayik, and P. Chomaz, Phys. Rev. C 63, 064305 (2001).
- [12] S. Yildirim, T. Gaitanos, M. Di Toro, and V. Greco, Phys. Rev. C 72, 064317 (2005).
- [13] Z.Y. Ma, N. Van Giai, A. Wandelt, D. Vretenar and P. Ring, Nucl. Phys. A 686, 173 (2001).
- [14] J. Piekarewicz, Phys. Rev. C 64, 024307 (2001).
- [15] J. Piekarewicz, Phys. Rev. C 66, 034305 (2002).
- [16] D. Vretenar, T. Nikšić, and P. Ring, Phys. Rev. C 68, 024310 (2003).
- [17] S. Shlomo and A. I. Sanzhur, Phys. Rev. C 65, 044310 (2002).
- [18] G. Colò and N. Van Giai, Nucl. Phys. A 731, 15 (2004).
- [19] H. L. Clark, Y.-W. Lui, and D. H. Youngblood, Phys. Rev. C 63, 031301(R) (2001).
- [20] D. H. Youngblood, Y.-W. Lui, B. John, Y. Tokimoto, H. L. Clark, and X. Chen, Phys. Rev. C 69, 054312 (2004).
- [21] G. Colò, N. Van Giai, P.F. Bortignon, and M.R. Quaglia, Phys. Lett. B 485, 362 (2000).
- [22] D. Vretenar, A. Wandelt, and P. Ring, Phys. Lett. B 487, 334 (2000).
- [23] S.I. Bastrukov, S. Misicu, and V.I. Sushkov, Nucl. Phys. A 562, 191 (1993).
- [24] S. Misicu, Phys. Rev. C 73, 024301 (2006).
- [25] D. Vretenar, N. Paar, P. Ring, and T. Nikšić, Phys. Rev. C 65, 021301(R) (2002).
- [26] M. Uchida et al., Phys. Lett. B 557, 12 (2003).
- [27] M. Uchida et al., Phys. Rev. C 69, 051301(R) (2004).

- [28] N. Paar, P. Ring, T. Nikšić and D. Vretenar, Phys. Rev. C 67, 034312 (2003).
- [29] G. A. Lalazissis, T. Nikšić, D. Vretenar, and P. Ring, Phys. Rev. C 71, 024312 (2005).
- [30] D. Vretenar, A. V. Afanasjev, G. A. Lalazissis, P. Ring, Phys. Rep. 409, 101 (2005).
- [31] D. H. Youngblood, Y.-W. Lui, and H. L. Clark, Phys. Rev. C 55, 2811 (1997).
- [32] D. H. Youngblood, H. L. Clark, and Y.-W. Lui, Phys. Rev. Lett. 82, 691 (1999).
- [33] D. H. Youngblood, Y.-W. Lui, H. L. Clark, B. John, Y. Tokimoto, and X. Chen, Phys. Rev. C 69, 034315 (2004).

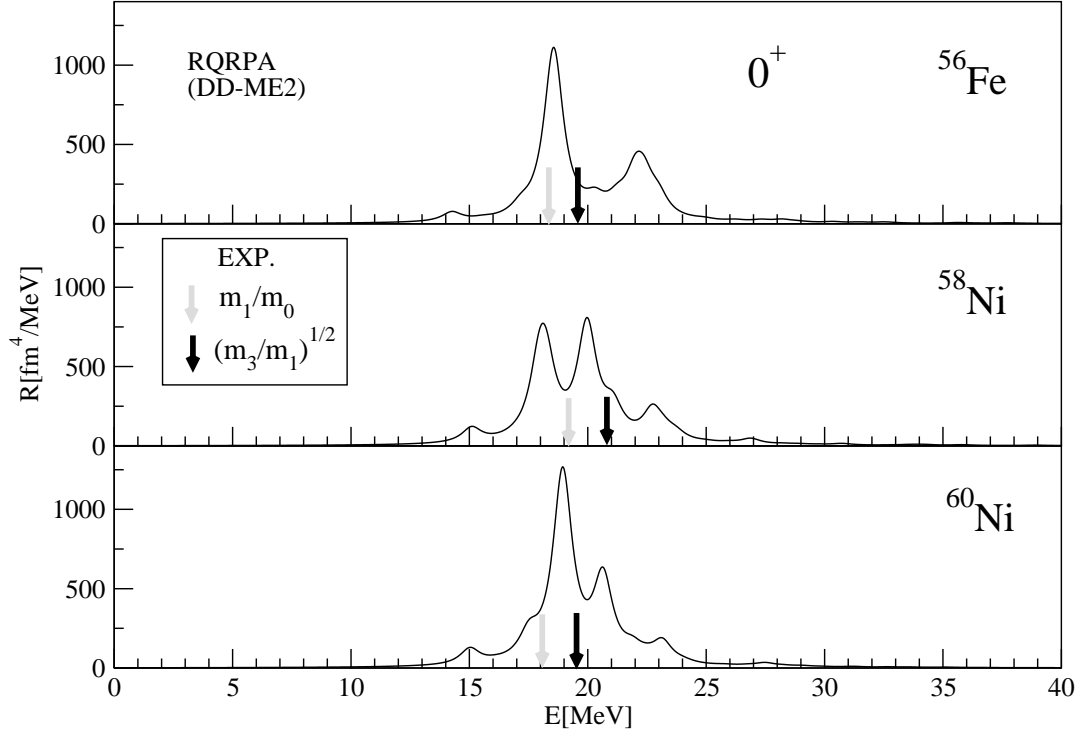


FIG. 1: The RHB+RQRPA isoscalar monopole strength distributions in  $^{56}\text{Fe}$ ,  $^{58}\text{Ni}$ , and  $^{60}\text{Ni}$  calculated with the density-dependent effective interaction DD-ME2. The experimental centroid ( $m_1/m_0$ ) and mean ( $\sqrt{m_3/m_1}$ ) energies obtained from  $(\alpha, \alpha')$  scattering [2] are denoted by grey and black arrows, respectively.

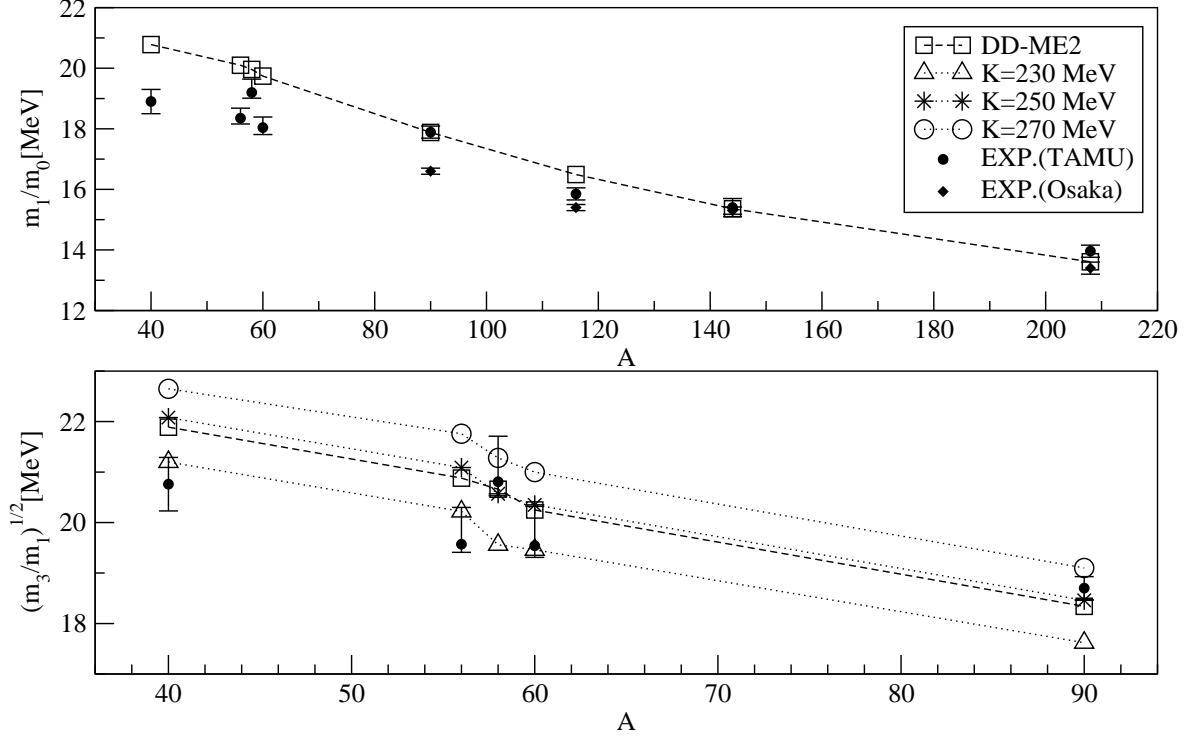


FIG. 2: In the mass region  $40 \leq A \leq 208$  the RQRPA results for the ISGMR centroid energies ( $m_1/m_0$ ), calculated with the relativistic DD-ME2 effective interaction, are plotted as a function of mass number and compared with data from the Texas A&M University (TAMU) [2, 31, 32, 33] and Osaka [26, 27] compilations (upper panel). In the lower panel the calculated ISGMR excitation energies  $\sqrt{m_3/m_1}$  for several medium-mass nuclei are shown in comparison with the data from Ref. [2]. In addition to the DD-ME2 interaction, three additional effective interactions with the values of the nuclear matter compressibility  $K_{nm}=230, 250,$  and  $270$  MeV [16] have been used in the RHB+RQRPA calculation of the ISGMR strength distributions.

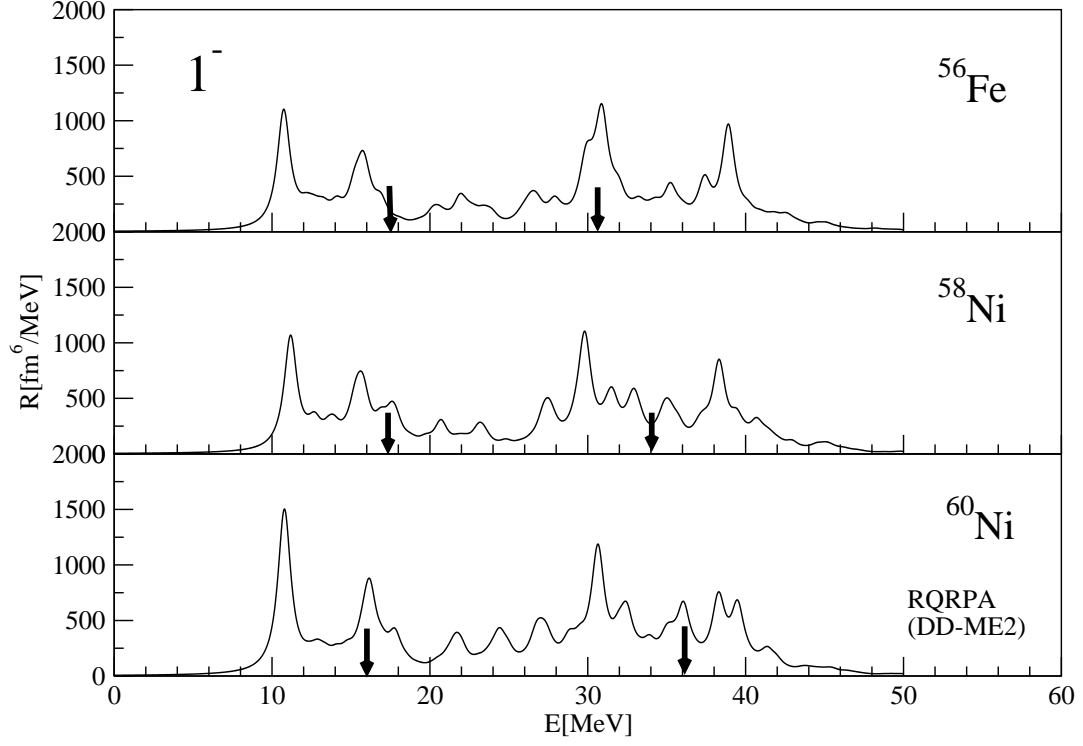


FIG. 3: The RHB+RQRPA isoscalar dipole transition strength in  $^{56}\text{Fe}$ ,  $^{58}\text{Ni}$ , and  $^{60}\text{Ni}$  calculated with DD-ME2 effective interaction. The arrows denote the positions of the experimental centroid energies of the low- and high-energy components [2].

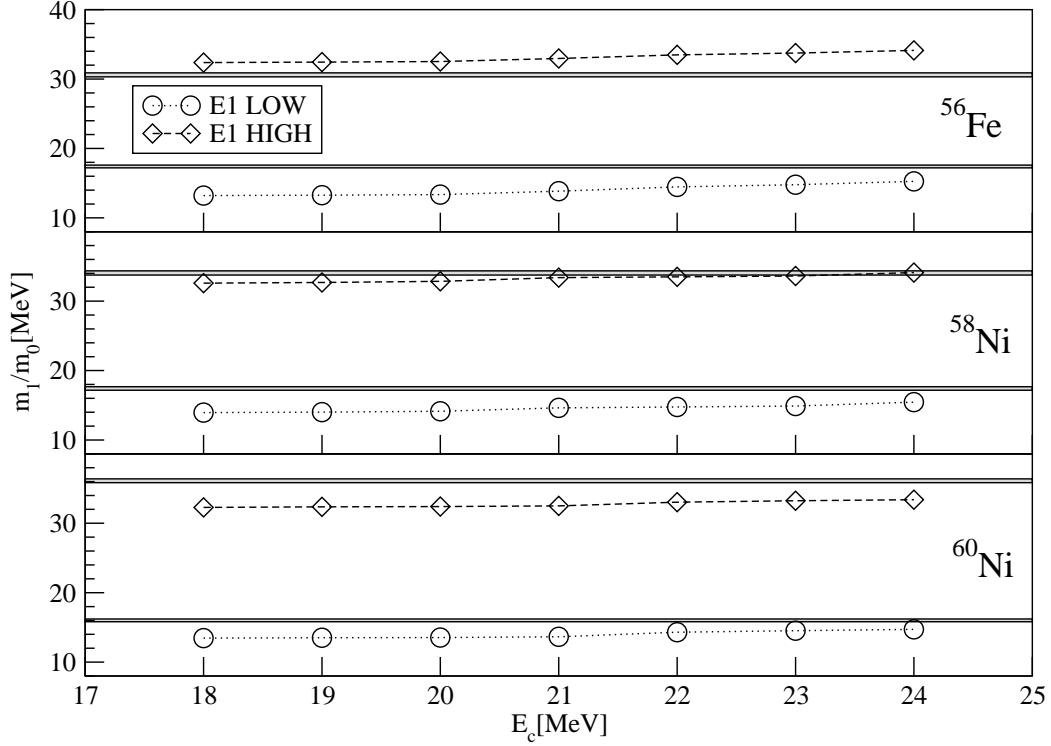


FIG. 4: Comparison of the RHB+RQRPA (circles and diamonds) and experimental (thick lines) [2] centroid energies of the low- and high-energy components of the isoscalar dipole transition strength in  $^{56}\text{Fe}$ ,  $^{58}\text{Ni}$ , and  $^{60}\text{Ni}$ . The results are plotted for different values of  $E_c$ , the parameter which separates the low- and high-energy regions.